

Gas-Phase Preparation of 1-Germavinylidene (H_2CGe ; X^1A_1), the Isovalent Counterpart of Vinylidene (H_2CC ; X^1A_1), via Non-adiabatic Dynamics through the Elementary Reaction of Ground State Atomic Carbon (C ; 3P) with Germane (GeH_4 ; X^1A_1)

Zhenghai Yang,[§] Bing-Jian Sun,[§] Chao He, Jin-Qi Li, Agnes H. H. Chang,* and Ralf I. Kaiser*



Cite This: *J. Phys. Chem. Lett.* 2023, 14, 430–436



Read Online

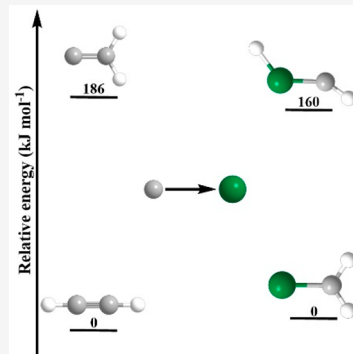
ACCESS |

Metrics & More

Article Recommendations

Supporting Information

ABSTRACT: 1-Germavinylidene (H_2CGe ; X^1A_1), the germanium analogue of vinylidene (H_2CC ; X^1A_1), was prepared via a directed gas-phase synthesis through the bimolecular reaction of ground state atomic carbon (C ; 3P) with germane (GeH_4 ; X^1A_1) under single-collision conditions. The reaction commences with the barrierless insertion of carbon into the Ge–H bond followed by intersystem crossing from the triplet to singlet surface and migration of atomic hydrogen to germylene (H_2GeCH_2), which predominantly decomposes via molecular hydrogen loss to 1-germavinylidene (H_2CGe ; X^1A_1). Therefore, the replacement of a single carbon atom in the acetylene–vinylidene system by germanium critically impacts the chemical bonding, molecular structure, and thermodynamic stability of the carbene-type structures favoring 1-germavinylidene (H_2CGe) over germyne ($HGeCH$) by 160 kJ mol⁻¹. Hence, the carbon–germane system represents a benchmark in the exploration of the chemistries of main group 14 elements with germanium-bearing systems showing few similarities with the isovalent carbon system.



The very first isolation of disilenes ($Si=Si$) in 1981 by West et al. challenged the conventional wisdom of the “double bond rule”,¹ i.e., a postulate that main group 14 elements heavier than carbon cannot form homo- and heteronuclear multiple bonds.^{2,3} As of today, stable compounds carrying homonuclear double bonds ($E=E$, where $E = Si$, Ge , Sn , or Pb)^{4–6} such as disilene, digermene, distannene, and diplumbene have been synthesized, and although more challenging, triply bonded compounds, including disilyne ($Si\equiv Si$),⁷ digermyne ($Ge\equiv Ge$),⁸ distannyne ($Sn\equiv Sn$),⁹ and diplumbyne ($Pb\equiv Pb$),¹⁰ were also isolated. These heavier analogues of alkynes ($E\equiv E$) display *trans*-bent geometries with decreased $R-E-E$ angles from 137.44° (disilyne) to 94.26° (diplumbyne) and decreased bond orders from silicon to lead culminating in nearly 90° bending angles and a formal single bond in diplumbynes ($RPbPbR$),¹⁰ marking a strong contrast to acetylene and its linear geometry.

As for the heteronuclear multiple bonds, an understanding of the chemical bonding of the chemistry of heteronuclear alkene analogues ($C=E$, where $E = Si$, Ge , or Pb)^{2,11–14} along with heteronuclear alkyne analogues involving the $C\equiv Si$ bond^{15–18} is beginning to emerge. For the H_2CGe isomers (Scheme 1), singlet 1-germavinylidene ($H_2C=Ge$) represents the global minimum; the simplest germyne ($HC\equiv GeH$), the *trans*-bent isomer, is less stable by ~160 kJ mol⁻¹.¹⁹ This strongly contrasts the carbon analogue acetylene ($HC\equiv CH$)–vinylidene ($H_2C=C$) system, with acetylene being more stable than vinylidene by 186 kJ mol⁻¹.^{19–21} Previous electronic

structure calculations revealed that the 1-germavinylidene (H_2CGe ; X^1A_1), germyne ($HGeCH$; X^1A'), and 2-germavinylidene ($CGeH_2$; X^1A_1) isomers are planar; nonclassical monobridged or dibridged isomers such as $Ge(\mu-H)SiH$ and $Ge(\mu-H_2)Si$ in the $SiGeH_2$ system do not represent local minima.²⁰ 1-Germavinylidene (H_2CGe) was first explored via electric discharge of tetramethylgermane in argon. Therein, the LIF (laser-induced fluorescence) spectra of 1-germavinylidene were obtained.²² After that, a series of studies were conducted focusing on 1-germavinylidene investigating the $B^1B_2-X^1A_1$ and $A^1A_2-X^1A_1$ transitions along with the corresponding vibrational frequencies of the ground and A states.^{23,24} However, compared to silynes ($R-Si\equiv Si-R$), the preparative synthesis of germynes ($R-Ge\equiv C-R$) has been poorly explored considering their high reactivity through dimerization leading to four-member ring structures.^{25,26} Even germynes with small substituents ($RC\equiv GeR$, where $R = F$, H , OH , CH_3 , or SiH_3) are extremely difficult to prepare.²⁶ In 2001, Bibal et al. reported the first synthesis of the germyne $Ar-Ge\equiv C-SiMe_3$ [$Ar = 2,4-di-tert-butyl-6-(diisopropylaminomethyl)phenyl$] as a

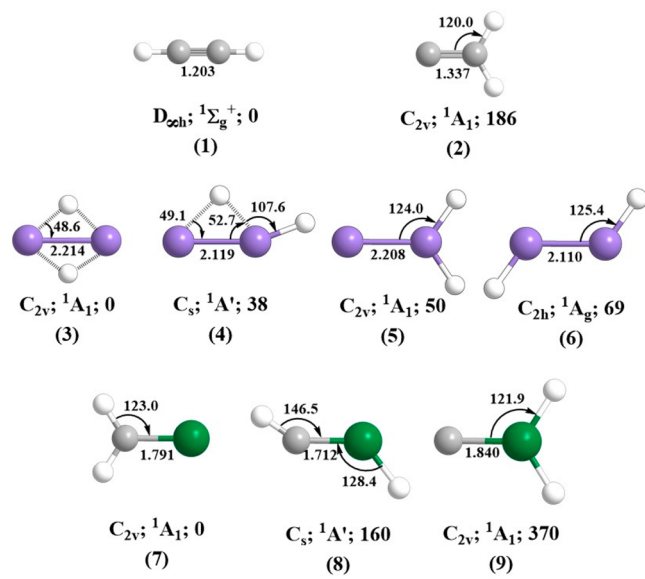
Received: December 9, 2022

Accepted: January 5, 2023

Published: January 9, 2023



Scheme 1. Molecular Geometries of H_2CC , H_2SiSi , and H_2CGe Isomers, Including Selected Bond Angles (degrees), Bond Distances (angstroms), Relative Energies (kilojoules per mole), Electronic States, and Point Groups



highly reactive intermediate.²⁷ In 2011, the isolation and characterization of the first persistent phosphine-stabilized germyne were accomplished (C-phosphino-Ge-aminogermyne).²⁸ However, the Ge–C bond length was determined to be 1.887 Å, which is longer than that (1.712 Å) for the germyne stem compound ($\text{HC}\equiv\text{GeH}$) ranging between that of a Ge–C bond (1.95–2.00 Å) and a Ge=C bond (1.77–1.83 Å). This has been interpreted through the effects of the electron-withdrawing and π -donating substituents.^{26,28} The electronic and steric effects of bulky substituents are best reflected in the reversed order of stability of substituted molecules with $\text{RC}\equiv\text{GeR}$ [$\text{R} = \text{Tbt}$ or $\text{SiMe}(\text{SiBu}_3)_2$] representing the global minimum.²⁶

The crossed molecular beam approach provides ideal experimental conditions for preparing exotic species, including 1-germavinylidene (H_2CGe) and germyne (HCGeH) through the reaction of ground state carbon ($\text{C}; ^3\text{P}$) with germane (GeH_4 ; X^1A_1) in the gas phase.^{29,30} Considering the single-collision conditions of the experiments, the bimolecular reaction products fly away undisturbed, thus excluding consecutive collisions such as dimerization and cycloaddition; these experimental conditions provide a universal, directed synthetic route to highly reactive germynes and germynes under controlled conditions considering that the hydrogen atom of the germane reactants can be substituted by any (in)organic functional group.^{5,26} Our experiments along with computational and statistical calculations suggest that singlet 1-germavinylidene (H_2CGe ; X^1A_1) represents the main product (50.97%) followed by germyne (HCGeH ; $\text{X}^1\text{A}'$; 18.88%) and 2-germavinylidene [CGeH_2 ; X^1A_1 ; 30.15% (Table S1)]. Our study reveals that the reaction commences with a barrierless insertion of atomic carbon into the Ge–H bond of germane followed by intersystem crossing (ISC) of the triplet intermediate germylmethylenes (HCGeH_3 ; $a^3\text{A}'$) to singlet germylmethylenes (HCGeH_3 ; X^1A). The latter undergoes facile hydrogen migration to germylene (H_2CGeH_2 ; X^1A_1), which either decomposes via molecular hydrogen loss to 1-

germavinylidene or undergoes another hydrogen shift to methylgermylene (CH_3GeH ; $\text{X}^1\text{A}'$) prior to unimolecular decomposition to 1-germavinylidene. These non-adiabatic reaction dynamics may serve as a universal template initiating advanced studies in the gas-phase preparation of highly reactive, dinuclear main group hydrides with various degrees of hydrogenation involving germanium for a better understanding of their chemical bonding and molecular structures at the molecular level.

The time-of-flight (TOF) spectra collected in the carbon–germane system were searched from m/z 92 (${}^{76}\text{GeCH}_4^+$) to m/z 84 (${}^{70}\text{GeCH}_2^+$) accounting for the natural isotope abundance of carbon [${}^{12}\text{C}$ (98.9%), ${}^{13}\text{C}$ (1.1%)] and germanium [${}^{70}\text{Ge}$ (20.5%), ${}^{72}\text{Ge}$ (27.4%), ${}^{73}\text{Ge}$ (7.8%), ${}^{74}\text{Ge}$ (36.7%), ${}^{76}\text{Ge}$ (7.8%)]. The best signal was observed at m/z 88 ($\text{C}{}^{74}\text{GeH}_2^+/\text{C}{}^{73}\text{GeH}_3^+/{}^{13}\text{C}{}^{74}\text{GeH}^+/{}^{13}\text{C}{}^{73}\text{GeH}_2^+/\text{C}{}^{76}\text{Ge}$) with ion counts at m/z 89 ($\text{C}{}^{74}\text{GeH}_3^+/{}^{13}\text{C}{}^{74}\text{GeH}_2^+/{}^{13}\text{C}{}^{73}\text{GeH}_3^+/\text{C}{}^{76}\text{GeH}/{}^{13}\text{C}{}^{76}\text{Ge}$) accumulated at a level of only $16 \pm 3\%$. No definite signal could be detected at m/z 91 or 92, indicating that no CGeH_4 adducts survive the flight time from the interaction region to the electron impact ionizer within our detector. The signal at m/z 88 can be best fit with a single channel via molecular hydrogen elimination and the preparation of CGeH_2 (88 amu) (Figure 1). The signal at lower mass-to-charge ratios originates predominantly from dissociative ionization of the neutral product. It should be noted that the dicarbon (C_2) and tricarbon (C_3) were also produced in the experiment; under our experimental conditions, their contribution could be minimized to <5%. However, no signal at higher masses was detectable, suggesting that neither dicarbon nor tricarbon accounts for the reactive scattering signal at m/z 88. The LAD (laboratory angular distribution) is spread at least over 50° from 17° to 65° with a maximum around the CM angle of 53.3 ± 0.6° (Figure 1). These findings propose indirect scattering dynamics and the formation of the long-lived CGeH_4 complex(es), which can fragment to CGeH_2 isomer(s) through molecular hydrogen loss.

To elucidate the underlying reaction mechanisms, the experimental data (TOFs and LAD) were transformed from the laboratory to the CM reference frame. The experimental data were replicated with a single molecular loss channel with a mass combination of m/z 88 (H_2CGe) and m/z 2 (H_2). It should be noted that all attempts to fit the laboratory data with an atomic hydrogen loss channel failed. Figure 2 depicts the resulting center of mass translational and angular flux distributions, $P(E_T)$ and $T(\theta)$, respectively, of the best fits. Upon inspection of the CM functions, the $P(E_T)$ reveals a maximum translation energy E_{\max} of $302 \pm 22 \text{ kJ mol}^{-1}$, which corresponds to the sum of the collision energy ($35.5 \pm 1.2 \text{ kJ mol}^{-1}$) and the reaction exoergicity for those products formed without internal excitation. Hence, a reaction energy of $-266 \pm 23 \text{ kJ mol}^{-1}$ is derived. In addition, the $P(E_T)$ displays a most probable energy of $32 \pm 2 \text{ kJ mol}^{-1}$, suggesting a tight exit transition state of the unimolecular decomposition of the CGeH_4 intermediate(s) to the final products. Also, $T(\theta)$ is forward–backward symmetric with respect to the distribution minimum at 90° (Figure 2). These findings propose indirect reaction dynamics with the long-lived CGeH_4 intermediates (lifetime longer than or comparative to that of the rotational period) and geometrical constraints of the decomposing complex(es) with molecular hydrogen emitted nearly within

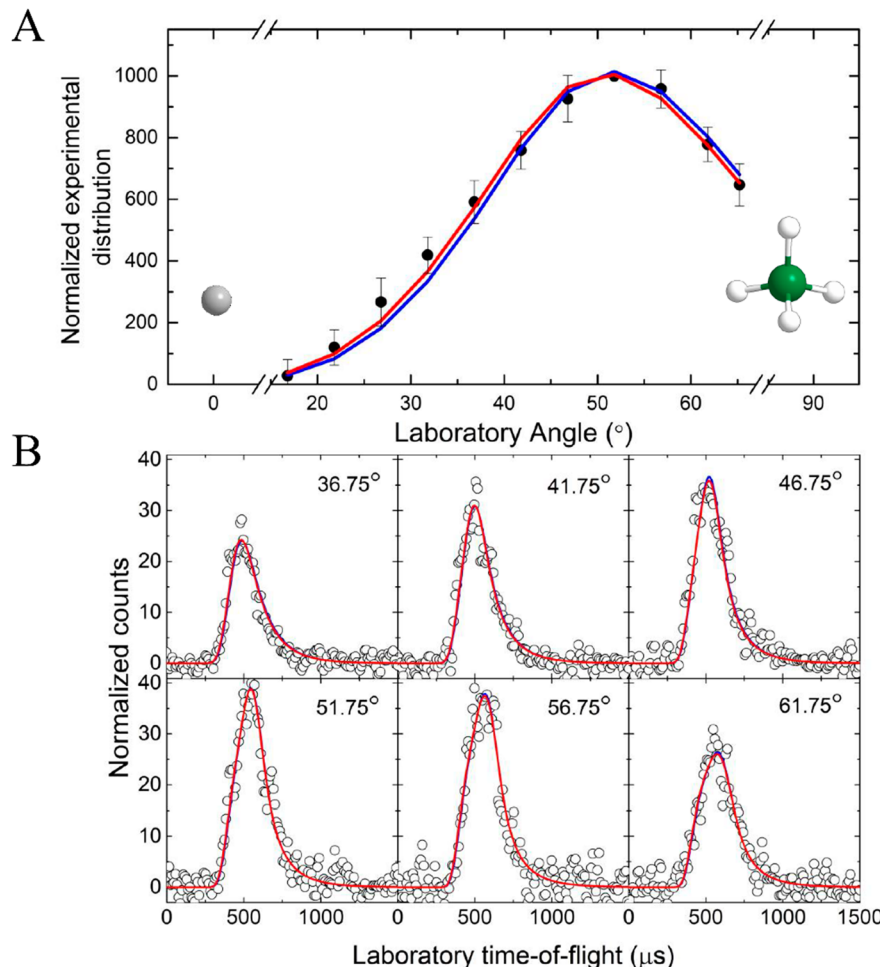


Figure 1. (A) LAD and (B) TOFs recorded in the $\text{C}-\text{GeH}_4$ reaction at m/z 88. The filled circles with their error bars represent the normalized experimental distribution; the empty circles indicate the experimental data. The red lines represent the best fits obtained with the $\text{C} + ^{74}\text{GeH}_4 \rightarrow \text{C}^{74}\text{GeH}_2 + \text{H}_2$ reaction channel, and the blue line represents the $\text{C} + ^{76}\text{GeH}_4 \rightarrow \text{C}^{76}\text{GeH}_2 + \text{H}_2$ reaction channel. Atom colors: carbon, gray; germanium, green; and hydrogen, white.

the rotational plane of the decomposing intermediate nearly perpendicular to the total angular momentum vector.³¹

Our experimental data unravel an exoergic molecular hydrogen loss channel with a reaction energy of -266 ± 23 kJ mol⁻¹ through indirect reaction dynamics. We combine these experimental results now with electronic structure calculation results to explore the underlying mechanisms and to determine the structural isomer(s) formed (Figure 3 and Figure S1). Our calculation revealed three singlet (¹p5–¹p7) and three triplet CGeH₂ isomers (³p5–³p7). 1-Germavinyldiene (H_2CGe ; X¹A₁; ¹p7) with a germanium–carbon π bond represents the most stable isomer on the singlet surface followed by *trans*-bent germyne (HCGeH ; X¹A'; ¹p6) and 2-germavinyldiene (CGeH_2 ; X¹A₁; ¹p5). The H₂CGe, HCGeH, CGeH₂ order of stability of the singlet species mirrors the triplet isomers with the latter less stable by 20–150 kJ mol⁻¹. This sequence of stability agrees well with previous calculations.^{19,32} How can these products be formed? The calculations reveal that the reaction of ground state atomic carbon (³P) with germane (X¹A₁) is initiated on the triplet surface via barrierless insertion of carbon into one of the four germanium–hydrogen bonds forming triplet germylmethylenes (HCGeH_3 ; a³A; ³i1) residing 322 kJ mol⁻¹ below the separated reactants. ³i1 can undergo unimolecular decom-

position to triplet *trans*-bent isomer ³p6 (HCGeH ; triplet germyne; a³A'') via the elimination of molecular hydrogen from the germyl group through a barrier of 217 kJ mol⁻¹ or isomerizes to ³i2 (H_2CGeH_2 ; a³A''; triplet germylene) via hydrogen migration. The transition state connecting ³i1 and ³p5 (CGeH_2 ; triplet 2-germavinyldiene) is located 43 kJ mol⁻¹ above the separated reactants; considering our collision energy, this transition state cannot be overcome under our experimental conditions. Once formed on the triplet surface, ³i2 can dissociate to ³p6 and ³p7 through molecular hydrogen loss channels or undergoes a hydrogen atom shift from germanium to carbon yielding the most stable intermediate on the triplet surface, ³i3 (H_3CGeH ; methylgermylene; a³A''), followed by molecular hydrogen ejection; this results in the formation of ³p7 (H_2CGe ; triplet 1-germavinyldiene; a³A₂) or ³p6.

How might singlet isomers ¹p5–¹p7 be formed? ³i1 is predicted to undergo ISC to singlet ¹i1 (germethylmethylene; X¹A; HCGeH_3) with the seam of crossing (MSX) reflecting a geometry similar to that of ¹i1; this MSX ranges 78 kJ mol⁻¹ above ³i1, but only 13 kJ mol⁻¹ above ¹i1. Two reaction channels can be accessed from ¹i1, namely, unimolecular decomposition to ¹p6 or isomerization to ¹i2 (H_2CGeH_2 ; X¹A₁; germylene) via hydrogen migration. In addition to

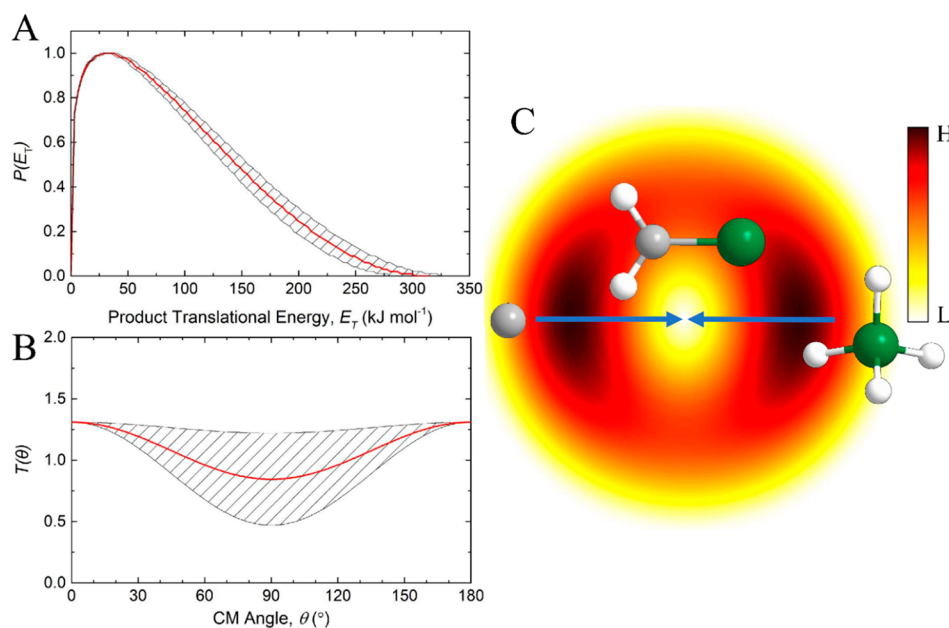


Figure 2. (A) CM translational energy, (B) angular flux distributions, and (C) corresponding flux contour map for the C–GeH₄ system. The red lines represent the best fit; shaded areas depict the error limits of the best fits.

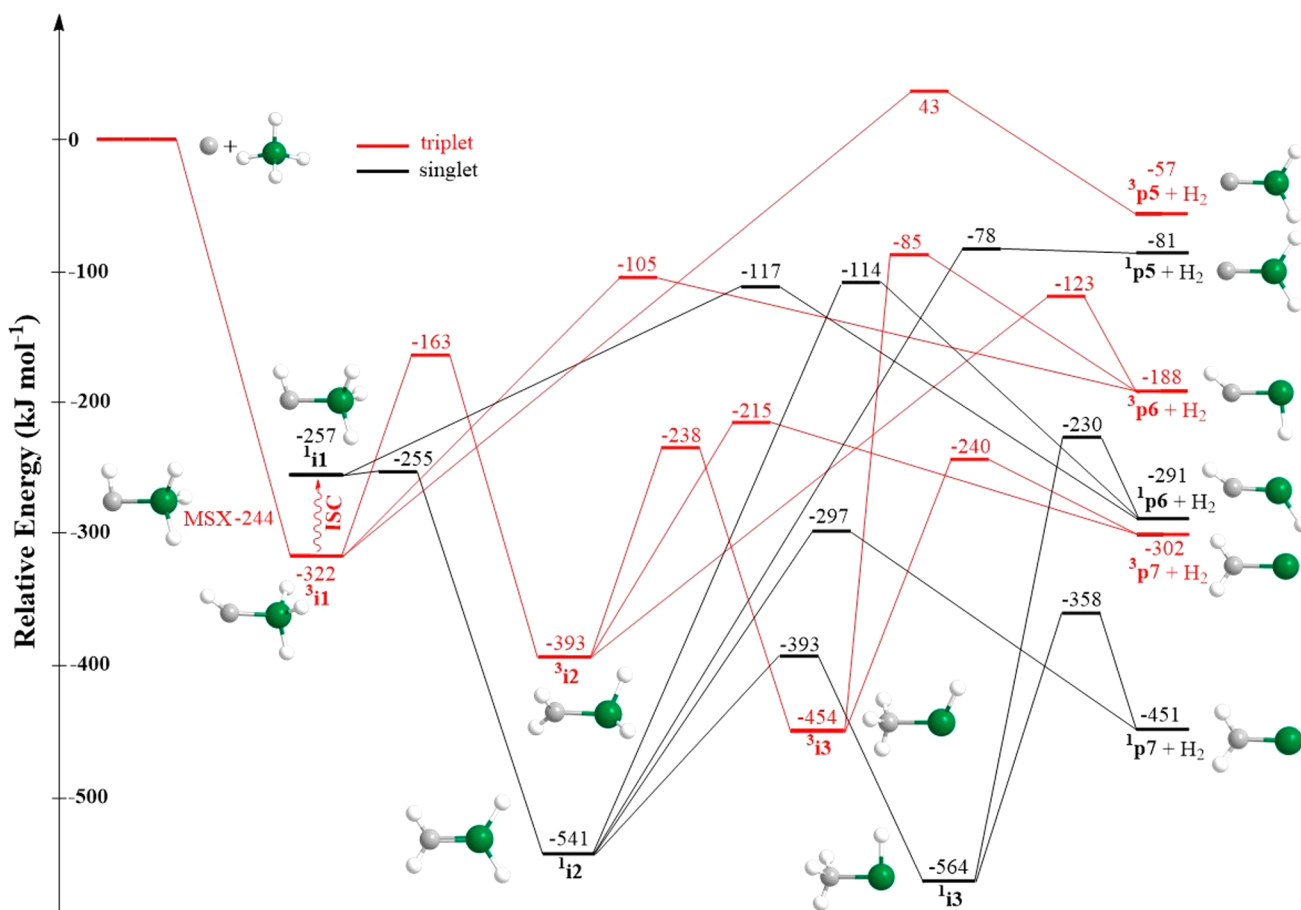


Figure 3. Triplet (red) and singlet (black) molecular hydrogen loss pathways of the C (³P)–GeH₄ (X¹A₁) system.

isomerization to ¹i3 (methylgermylene; X¹A'; H₃CGeH), the loss of molecular hydrogen from germanium of ¹i2 leads to ¹p7, whereas elimination of molecular hydrogen from carbon results in ¹p5; cleavage of the C–H and Ge–H bonds forms

¹p6. Finally, ¹p7 and ¹p6 can also be accessed from ¹i3, the most stable structure on the PES. Therefore, two reaction routes commencing with ¹i1 to the thermodynamically most stable product, 1-germavinylidene (¹p7), are identified on the

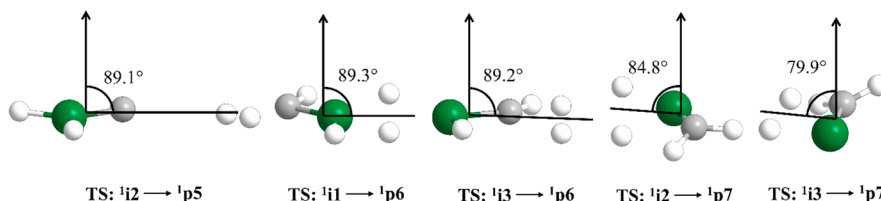


Figure 4. Calculated geometries of the exit transition states resulting in ${}^1\text{p}5 - {}^1\text{p}7$.

singlet surface, including ${}^1\text{i}1 \rightarrow {}^1\text{i}2 \rightarrow {}^1\text{i}3 \rightarrow {}^1\text{p}7$ and ${}^1\text{i}1 \rightarrow {}^1\text{i}2 \rightarrow {}^1\text{p}7$. Three routes to ${}^1\text{p}6$ are revealed computationally, namely, ${}^1\text{i}1 \rightarrow {}^1\text{p}6$, ${}^1\text{i}1 \rightarrow {}^1\text{i}2 \rightarrow {}^1\text{p}6$, and ${}^1\text{i}1 \rightarrow {}^1\text{i}2 \rightarrow {}^1\text{i}3 \rightarrow {}^1\text{p}6$; one pathway is assigned to ${}^1\text{p}5$, i.e., ${}^1\text{i}1 \rightarrow {}^1\text{i}2 \rightarrow {}^1\text{p}5$.

Which are the dominating reaction products? A comparison of the experimentally derived reaction exoergicity of 266 ± 23 kJ mol $^{-1}$ with the computational reaction energies (Figure 3) suggests that the formation of three isomers (${}^3\text{p}6$, ${}^1\text{p}5$, and ${}^3\text{p}5$) can be excluded because the reactions are exoergic by only 188 ± 8 , 81 ± 8 , and 57 ± 8 kJ mol $^{-1}$, respectively. However, synthesis of the three remaining structures (${}^1\text{p}7$, ${}^3\text{p}7$, and ${}^1\text{p}6$) should be reflected in reaction energies of 451 ± 8 , 302 ± 8 , and 291 ± 8 kJ mol $^{-1}$, respectively, which are clearly higher than the experimentally derived value of 266 ± 23 kJ mol $^{-1}$. Therefore, ${}^1\text{p}7$, ${}^3\text{p}7$, and/or ${}^1\text{p}6$ must be formed in a highly rovibrationally excited state. As observed recently in the dicarbon–silane³³ and methylidyne–dimethylacetylene systems,³⁴ this would shift the maximum translational energy release to lower values, thus providing a rationale for the discrepancy between the computed reaction energies and the experimentally derived data. We can utilize the theoretically predicted structures of the exit transition states of the molecular hydrogen losses to ${}^3\text{p}7$ and ${}^1\text{p}5 - {}^1\text{p}7$ to narrow down potential products even further. Recall that the center-of-mass angular distribution reveals that the molecular hydrogen loss commences nearly within the rotational plane of the decomposing complex. A detailed inspection of the geometries of these exit transition states reveals that among the possible products, only singlet species ${}^1\text{p}5 - {}^1\text{p}7$ fulfill this requirement for transition states ${}^1\text{i}2 \rightarrow {}^1\text{p}5$ (0.9°), ${}^1\text{i}3 \rightarrow {}^1\text{p}6$ (0.8°), ${}^1\text{i}1 \rightarrow {}^1\text{p}6$ (0.7°), ${}^1\text{i}2 \rightarrow {}^1\text{p}7$ (5.2°), and ${}^1\text{i}3 \rightarrow {}^1\text{p}7$ (10.1°) (Figure 4). This finding also proposes that ISC from the triplet to the singlet manifold is rapid with non-adiabatic dynamics dictating the ${}^3\text{i}1 \rightarrow {}^1\text{i}1$ pathway followed by a rapid hydrogen shift through a barrier of only 2 kJ mol $^{-1}$ to ${}^1\text{i}2$. The favorable ISC can also be understood in terms of the heavy atom effect (germanium) and the fact that the competing ${}^3\text{i}1 \rightarrow {}^3\text{i}2$ pathway is unfavorable considering the barrier of 159 kJ mol $^{-1}$ for the atomic hydrogen shift.

Considering the five remaining pathways (${}^1\text{i}2 \rightarrow {}^1\text{p}5$, ${}^1\text{i}2 \rightarrow {}^1\text{p}6$, ${}^1\text{i}2 \rightarrow {}^1\text{p}7$, ${}^1\text{i}2 \rightarrow {}^1\text{i}3 \rightarrow {}^1\text{p}6$, and ${}^1\text{i}2 \rightarrow {}^1\text{i}3 \rightarrow {}^1\text{p}7$), a close inspection of the energies of the transition states reveals that the formation of 1-germavinylidene (${}^1\text{p}7$) is favorable. This conclusion also gains full support from Rice–Ramsperger–Kassel–Marcus (RRKM) calculations and the dominating formation of 1-germavinylidene [${}^1\text{p}7$, 50.97% (Table S1)] compared to *trans*-bent germyne (${}^1\text{p}6$, 18.88%) and 2-germavinylidene (${}^1\text{p}5$, 30.15%) (Supporting Information), thus providing an elegant route to the gas-phase preparation of 1-germavinylidene (${}^1\text{p}7$) under single-collision conditions via non-adiabatic reaction dynamics. This pathway is also favorable compared to a potential atomic hydrogen loss to form methylgermylidene ($\text{CH}_3\text{Ge}; {}^2\text{A}$) via the ${}^1\text{i}2 \rightarrow {}^1\text{i}3 \rightarrow$

${}^2\text{p}4$ pathway (Figure S1) as evidenced through the non-experimental detection of the atomic hydrogen loss pathway.

Overall, utilizing the crossed molecular beam machine combined with electronic structure and statistical calculations, our study marks the first directed gas-phase formation of 1-germavinylidene ($\text{H}_2\text{CGe}; {}^3\text{A}_1$) via the elementary reaction of the ground state carbon ($\text{C}; {}^3\text{P}$) with germane ($\text{GeH}_4; {}^3\text{A}_1$), the simplest closed-shell germanium–hydrogen bonds leading to triplet germylmethylene ($\text{HCGeH}_3; {}^3\text{A}$). The latter undergoes rapid intersystem crossing to the singlet manifold and singlet germylmethylene ($\text{HCGeH}_3; {}^1\text{A}$), which then isomerizes nearly instantaneously through a hydrogen shift to germylene ($\text{H}_2\text{CGeH}_2; {}^1\text{A}_1$) followed by either decomposition via molecular hydrogen loss to afford 1-germavinylidene ($\text{H}_2\text{CGe}; {}^1\text{A}_1$) or another hydrogen shift to afford methylgermylene ($\text{CH}_3\text{GeH}; {}^1\text{A}'$) prior to unimolecular decomposition to 1-germavinylidene ($\text{H}_2\text{CGe}; {}^1\text{A}_1$). The preparation of the unstable molecules with multiple bonds has been studied utilizing various methods, including laser flash photolysis,³⁵ matrix isolation,³² electric discharge,²² and vacuum gas–solid reactions.³⁶ However, directed gas-phase preparation of extremely unstable molecules and determination of the corresponding angular distribution and translational energy information without consecutive collisions and wall effects are still needed. Here, our findings demonstrate the unique potential of crossed molecular beam experiments to prepare unstable, even highly unsaturated organometallic molecules in the gas phase, which cannot be accessed through classical preparative synthetic methods.^{25,26}

METHODS

Experimental Section. The $\text{C}-\text{GeH}_4$ reaction was performed at the University of Hawaii.³⁷ The helium-seeded supersonic beam of ground state atomic carbon was prepared via ablation of a graphite rod.³⁸ The pulsed carbon beam was characterized by a peak velocity v_p of 2560 ± 52 m s $^{-1}$. The primary carbon beam crossed perpendicularly with a germane beam ($v_p = 531 \pm 5$ m s $^{-1}$) leading to a center-of-mass (CM) angle of $53.3 \pm 0.6^\circ$ and a collision energy of 35.5 ± 1.2 kJ mol $^{-1}$ (Table S2). The reactively scattered products were monitored via a rotatable detector under ultra-high-vacuum conditions (8×10^{-12} Torr). The TOF spectra were collected at different angles between 17° and 65° with respect to the primary beam. These laboratory data were converted via forward convolution to the CM frame yielding the CM translational energy [$P(E_T)$] and angular [$T(\theta)$] flux distributions, along with information about the reaction dynamics.^{31,39}

Computational Studies. The geometries of species along H and H_2 loss channels on adiabatic ground state singlet and triplet potential surfaces are optimized via the coupled

cluster^{40,41} CCSD/cc-pVTZ calculations (some with MP2/cc-pVTZ) (**Tables S3 and S4**). Their energies are refined to complete basis set limits⁴² [CCSD(T)/CBS] with CCSD/cc-pVTZ (some with MP2/cc-pVTZ) zero-point energy corrections, which are derived by extrapolating the CCSD(T)/cc-pVTZ, CCSD(T)/cc-pVDZ, and CCSD(T)/cc-pVQZ energies. The ³i1 and ¹i1 minimum-energy crossing point is located by employing CPMSCF/TZVPP calculation, and the corresponding CCSD(T)/CBS energy is also obtained. MOLPRO⁴³ and GAUSSIAN16⁴⁴ were utilized in the surface crossing and coupled cluster calculations, respectively. Moreover, the energy-dependent RRKM rate constants⁴⁵ are then calculated on the basis of CCSD/cc-pVTZ harmonic frequencies and zero-point-corrected CCSD(T)/CBS energies. The saddle-point approach^{45,46} is used to compute the number of states for transition states and the density of states for intermediates. Note that all of the species are considered as a collection of harmonic oscillators. Eventually, the product branching ratios are estimated by solving the *ab initio* reaction path-based rate equations with the numerical Runge–Kutta method.

ASSOCIATED CONTENT

Supporting Information

The Supporting Information is available free of charge at <https://pubs.acs.org/doi/10.1021/acs.jpcllett.2c03749>.

Detailed experimental and computational methods, atomic hydrogen loss pathways of the C–GeH₄ reaction (Figure S1), computed RRKM results (Table S1), experimental parameters (Table S2), vibrational frequencies and infrared intensities (Table S3), and optimized coordinate structures involved in the C–GeH₄ reaction (Table S4) ([PDF](#))

AUTHOR INFORMATION

Corresponding Authors

Ralf I. Kaiser – Department of Chemistry, University of Hawai'i at Manoa, Honolulu, Hawaii 96822, United States; orcid.org/0000-0002-7233-7206; Email: ralfk@hawaii.edu

Agnes H. H. Chang – Department of Chemistry, National Dong Hwa University, Hualien 974, Taiwan; Email: hhchang@gms.ndhu.edu.tw

Authors

Zhenghai Yang – Department of Chemistry, University of Hawai'i at Manoa, Honolulu, Hawaii 96822, United States

Bing-Jian Sun – Department of Chemistry, National Dong Hwa University, Hualien 974, Taiwan

Chao He – Department of Chemistry, University of Hawai'i at Manoa, Honolulu, Hawaii 96822, United States

Jin-Qi Li – Department of Chemistry, National Dong Hwa University, Hualien 974, Taiwan

Complete contact information is available at:

<https://pubs.acs.org/10.1021/acs.jpcllett.2c03749>

Author Contributions

[§]Z.Y. and B.-J.S. contributed equally to this work.

Notes

The authors declare no competing financial interest.

ACKNOWLEDGMENTS

The work at the University of Hawaii was supported by the U.S. National Science Foundation (CHE-1853541). B.-J.S., J.-Q.L., and A.H.H.C. thank the National Center for High-performance Computer in Taiwan for providing the computer resources.

REFERENCES

- West, R.; Fink, M. J.; Michl, J. Tetramesityldisilene, A Stable Compound Containing a Silicon-Silicon Double Bond. *Science* **1981**, *214*, 1343–1344.
- Weetman, C. Main Group Multiple Bonds for Bond Activations and Catalysis. *Chem. - Eur. J.* **2021**, *27*, 1941–1954.
- Bonnefille, E.; Mazières, S.; Saffon, N.; Couret, C. Reactivity of a Germa-Alkyne: Evidence for a Germanone Intermediate in the Hydrolysis and Alcoholytic Processes. *J. Organomet. Chem.* **2009**, *694*, 2246–2251.
- Fischer, R. C.; Power, P. P. π -Bonding and the Lone Pair Effect in Multiple Bonds Involving Heavier Main Group Elements: Developments in the New Millennium. *Chem. Rev.* **2010**, *110*, 3877–3923.
- Power, P. P. π -Bonding and the Lone Pair Effect in Multiple Bonds between Heavier Main Group Elements. *Chem. Rev.* **1999**, *99*, 3463–3504.
- Präsang, C.; Scheschkewitz, D. Reactivity in the Periphery of Functionalised Multiple Bonds of Heavier Group 14 Elements. *Chem. Soc. Rev.* **2016**, *45*, 900–921.
- Sekiguchi, A.; Kinjo, R.; Ichinohe, M. A Stable Compound Containing a Silicon-Silicon Triple Bond. *Science* **2004**, *305*, 1755–1757.
- Stender, M.; Phillips, A. D.; Wright, R. J.; Power, P. P. Synthesis and Characterization of a Digermanium Analogue of an Alkyne. *Angew. Chem., Int. Ed.* **2002**, *41*, 1785–1787.
- Phillips, A. D.; Wright, R. J.; Olmstead, M. M.; Power, P. P. Synthesis and Characterization of 2, 6-Dipp₂H₃C₆SnSnC₆H₃-2, 6-Dipp₂ (Dipp = C₆H₃-2, 6-Pri₂): A Tin Analogue of an Alkyne. *J. Am. Chem. Soc.* **2002**, *124*, 5930–5931.
- Pu, L.; Twamley, B.; Power, P. P. Synthesis and Characterization of 2, 6-Trip₂H₃C₆PbPbC₆H₃-2, 6-Trip₂ (Trip = C₆H₂-2, 4, 6-i-Pr₃): A Stable Heavier Group 14 Element Analogue of an Alkyne. *J. Am. Chem. Soc.* **2000**, *122*, 3524–3525.
- Brook, A. G.; Abdesaken, F.; Gutekunst, B.; Gutekunst, G.; Kallury, R. K. A Solid Silaethene: Isolation and Characterization. *J. Chem. Soc., Chem. Commun.* **1981**, 191–192.
- Lee, V. Y.; Sekiguchi, A. Heteronuclear Heavy Alkenes E = E' (E, E' = Group 14 Elements): Germasilenes, Silastannenes, Germastannenes... Next Stop? *Organometallics* **2004**, *23*, 2822–2834.
- Ottosson, H.; Eklöf, A. M. Silenes: Connectors between Classical Alkenes and Nonclassical Heavy Alkenes. *Coord. Chem. Rev.* **2008**, *252*, 1287–1314.
- Leung, W.-P.; Chan, Y.-C.; So, C.-W. Chemistry of Heavier Group 14 Base-Stabilized Heterovinylidenes. *Organometallics* **2015**, *34*, 2067–2085.
- Karni, M.; Apeloig, Y.; Schröder, D.; Zummack, W.; Rabezzana, R.; Schwarz, H. HCSiF and HCSiCl: The First Detection of Molecules with Formal C≡Si Triple Bonds. *Angew. Chem., Int. Ed.* **1999**, *38*, 331–335.
- Danovich, D.; Ogliaro, F.; Karni, M.; Apeloig, Y.; Cooper, D. L.; Shaik, S. Silynes (RC≡SiR') and Disilynes (RSi≡SiR'): Why Are Less Bonds Worth Energetically More? *Angew. Chem., Int. Ed.* **2001**, *40*, 4023–4026.
- Lühmann, N.; Müller, T. A Compound with a Si–C Triple Bond. *Angew. Chem., Int. Ed.* **2010**, *49*, 10042–10044.
- Gau, D.; Kato, T.; Saffon-Merceron, N.; De Cárzar, A.; Cossío, F. P.; Baceiredo, A. Synthesis and Structure of a Base-Stabilized C-Phosphino-Si-Amino Silyne. *Angew. Chem., Int. Ed.* **2010**, *49*, 6585–6588.

- (19) Hao, Q.; Lu, T.; Wilke, J. J.; Simonett, A. C.; Yamaguchi, Y.; Fang, D.-C.; Schaefer, H. F. 1-Germavinylidene ($\text{Ge} = \text{CH}_2$), Germyne (HGeCH), and 2-Germavinylidene ($\text{H}_2\text{Ge} = \text{C}$) Molecules and Isomerization Reactions among Them: Anharmonic Rovibrational Analyses. *J. Phys. Chem. A* **2012**, *116*, 4578–4589.
- (20) Boone, A. J.; Magers, D. H.; Leszczyński, J. Searches on the Potential Energy Hypersurfaces of GeCH_2 , GeSiH_2 , and Ge_2H_2 . *Int. J. Quantum Chem.* **1998**, *70*, 925–932.
- (21) Lee, H.; Baraban, J. H.; Field, R. W.; Stanton, J. F. High-Accuracy Estimates for the Vinylidene-Acetylene Isomerization Energy and the Ground State Rotational Constants of $\text{C} = \text{CH}_2$. *J. Phys. Chem. A* **2013**, *117*, 11679–11683.
- (22) Harper, W. W.; Ferrall, E. A.; Hilliard, R. K.; Stogner, S. M.; Grev, R. S.; Clouthier, D. J. Laser Spectroscopic Detection of the Simplest Unsaturated Silylene and Germylene. *J. Am. Chem. Soc.* **1997**, *119*, 8361–8362.
- (23) Hostutler, D. A.; Clouthier, D. J.; Pauls, S. W. The Ground State of Germylidene ($\text{H}_2\text{C} = \text{Ge}$). *J. Chem. Phys.* **2002**, *116*, 1417–1423.
- (24) He, S.-G.; Tackett, B. S.; Clouthier, D. J. A Stimulated Emission Pumping Study of the First Excited Singlet State of Germylidene ($\text{H}_2\text{C} = \text{Ge}$). *J. Chem. Phys.* **2004**, *121*, 257–264.
- (25) Xu, J.; Zheng, H.-f.; Liu, W.; Ding, Y.-h. A Motif for Heteronuclear $\text{C}\equiv\text{E}$ ($\text{E} = \text{Si}, \text{Ge}, \text{Sn}, \text{Pb}$) Bonding: Lewis Acid–Base Pair Strategy. *Phys. Chem. Chem. Phys.* **2020**, *22*, 26720–26727.
- (26) Wu, P.-C.; Su, M.-D. Theoretical Designs for Germaacetylene ($\text{RC}\equiv\text{GeR}'$): A New Target for Synthesis. *Dalton Trans.* **2011**, *40*, 4253–4259.
- (27) Bibal, C.; Mazières, S.; Gornitzka, H.; Courret, C. A Route to a Germanium–Carbon Triple Bond: First Chemical Evidence for a Germyne. *Angew. Chem., Int. Ed.* **2001**, *40*, 952–954.
- (28) Berthe, J.; Garcia, J. M.; Ocaso, E.; Kato, T.; Saffon-Merceron, N.; De Cozar, A.; Cossío, F. P.; Baceiredo, A. Synthesis and Reactivity of a Phosphine-Stabilized Monogermanium Analogue of Alkynes. *J. Am. Chem. Soc.* **2011**, *133*, 15930–15933.
- (29) Kaiser, R. I. Experimental Investigation on the Formation of Carbon-Bearing Molecules in the Interstellar Medium via Neutral–Neutral Reactions. *Chem. Rev.* **2002**, *102*, 1309–1358.
- (30) Kaiser, R. I.; Mebel, A. M. On the Formation of Polyacetylenes and Cyanopolyacetylenes in Titan’s Atmosphere and Their Role in Astrobiology. *Chem. Soc. Rev.* **2012**, *41*, 5490–5501.
- (31) Levine, R. D. *Molecular reaction dynamics*; Cambridge University Press, 2005.
- (32) Kaiser, R. I.; Carrier, W.; Osamura, Y.; Mahfouz, R. M. Infrared Spectroscopic Detection of the Methylgermyl (H_2GeCH_3) Radical and Its Perdeuterated Counterpart in Low Temperature Matrices. *Chem. Phys. Lett.* **2010**, *492*, 226–234.
- (33) Rettig, A.; Head-Gordon, M.; Doddipatla, S.; Yang, Z.; Kaiser, R. I. Crossed Beam Experiments and Computational Studies of Pathways to the Preparation of Singlet Ethynylsilylene ($\text{HCCSiH}; \text{X}^1\text{A}'$): The Silacarbene Counterpart of Triplet Propargylene ($\text{HCCCH}; \text{X}^3\text{B}$). *J. Phys. Chem. Lett.* **2021**, *12*, 10768–10776.
- (34) He, C.; Fujioka, K.; Nikolayev, A. A.; Zhao, L.; Doddipatla, S.; Azyazov, V. N.; Mebel, A. M.; Sun, R.; Kaiser, R. I. A Chemical Dynamics Study of the Reaction of the Methyldyne Radical ($\text{CH}, \text{X}^2\Pi$) with dimethylacetylene ($\text{CH}_3\text{CCCH}_3, \text{X}^1\text{A}_{1g}$). *Phys. Chem. Chem. Phys.* **2021**, *24*, 578–593.
- (35) Becerra, R.; Walsh, R. What Have We Learnt About Heavy Carbenes through Laser Flash Photolysis Studies? *Phys. Chem. Chem. Phys.* **2007**, *9*, 2817–2835.
- (36) Gaumont, A. C.; Denis, J. M. Preparation, Characterization, and Synthetic Potential of Unstable Compounds Containing Phosphorus-Carbon Multiple Bonds. *Chem. Rev.* **1994**, *94*, 1413–1439.
- (37) Yang, Z.; Sun, B. J.; He, C.; Fatimah, S.; Chang, A. H. H.; Kaiser, R. I. Gas Phase Preparation of the Elusive Monobridged $\text{Ge}(\mu-\text{H})\text{GeH}$ Molecule through Nonadiabatic Reaction Dynamics. *Chem. - Eur. J.* **2022**, *28*, No. e202103999.
- (38) Yang, Z.; He, C.; Goettl, S. J.; Paul, D.; Kaiser, R. I.; Silva, M. X.; Galvão, B. R. Gas-Phase Preparation of Silyl Cyanide (SiH_3CN) via a Radical Substitution Mechanism. *J. Am. Chem. Soc.* **2022**, *144*, 8649–8657.
- (39) Yang, Z.; He, C.; Goettl, S.; Kaiser, R. I.; Azyazov, V. N.; Mebel, A. M. Directed Gas-Phase Formation of Aminosilylene ($\text{HSiNH}_2; \text{X}^1\text{A}'$): The Simplest Silicon Analogue of an Aminocarbene, under Single-Collision Conditions. *J. Am. Chem. Soc.* **2021**, *143*, 14227–14234.
- (40) Purvis, G. D., III; Bartlett, R. J. A Full Coupled-Cluster Singles and Doubles Model: The Inclusion of Disconnected Triples. *J. Chem. Phys.* **1982**, *76*, 1910–1918.
- (41) Hampel, C.; Peterson, K. A.; Werner, H.-J. A Comparison of the Efficiency and Accuracy of the Quadratic Configuration Interaction (QCISD), Coupled Cluster (CCSD), and Brueckner Coupled Cluster (BCCD) Methods. *Chem. Phys. Lett.* **1992**, *190*, 1–12.
- (42) Peterson, K. A.; Woon, D. E.; Dunning, T. H., Jr Benchmark Calculations with Correlated Molecular Wave Functions. IV. The Classical Barrier Height of the $\text{H} + \text{H}_2 \rightarrow \text{H}_2 + \text{H}$ Reaction. *J. Chem. Phys.* **1994**, *100*, 7410–7415.
- (43) Werner, H. J.; Knowles, P. J.; Knizia, G.; Manby, F. R.; Schütz, M.; Celani, P.; Korona, T.; Lindh, R.; Mitrushenkov, A.; Rauhut, G. *MOLPRO, version 2015.1, A Package of Ab Initio Programs*; University of Cardiff: Cardiff, U.K., 2015.
- (44) Frish, M. J.; Trucks, G. W.; Schlegel, H. B.; Scuseria, G. E.; Robb, M. A.; Cheeseman, J. R.; Scalmani, G.; Barone, V.; Petersson, G. A.; Nakatsuji, H. *Gaussian 16, Revision C. 01*; Gaussian, Inc.: Wallingford, CT, 2019.
- (45) Chang, A. H. H.; Mebel, A. M.; Yang, X.-M.; Lin, S. H.; Lee, Y. T. Ab initio/RRKM Approach toward the Understanding of Ethylene Photodissociation. *J. Chem. Phys.* **1998**, *109*, 2748–2761.
- (46) Eyring, H.; Lin, S. H.; Lin, S. M. *Basic Chemical Kinetics*; John Wiley & Sons Inc.: New York, 1980.

Recommended by ACS

Formation of Thioformic Acid (HCOSH)—The Simplest Thioacid—in Interstellar Ice Analogues

Jia Wang, Ralf I. Kaiser, et al.

DECEMBER 19, 2022
THE JOURNAL OF PHYSICAL CHEMISTRY A

READ

Reaction of $\text{O}^{(3\text{P})}$ with Carbon Disulfide: Kinetics and Products

Yuri Bedjanian,

OCTOBER 19, 2022
ACS EARTH AND SPACE CHEMISTRY

READ

Formation of a Resonance-Stabilized Radical Intermediate by Hydroxyl Radical Addition to Cyclopentadiene

Kacee L. Caster, Fabien Goulay, et al.

NOVEMBER 23, 2022
THE JOURNAL OF PHYSICAL CHEMISTRY A

READ

Multichannel Radical–Radical Reaction Dynamics of $\text{NO} +$ Propargyl Probed by Broadband Rotational Spectroscopy

Nureshan Dias, Arthur G. Suits, et al.

AUGUST 08, 2022
THE JOURNAL OF PHYSICAL CHEMISTRY A

READ

Get More Suggestions >